Contents lists available at SciVerse ScienceDirect

CIRP Annals Manufacturing Technology

Journal homepage: www.elsevier.com/locate/cirp

Raising by spinning

Iacopo M. Russo[a], Christopher J. Cleaver[a] (RA), Evripides G. Loukaides[b] (RA), Julian M. Allwood[a] (1)

[a]*Department of Engineering, University of Cambridge, UK.* [b]*Department of Mechanical Engineering, University of Bath, UK.*

Industrial metal spinning depends on costly trial-and-error when introducing new products. However, a recently developed flexible spinning setup allows a new form of process operation similar to raising by hammering: two rollers on either side of the rotating workpiece apply a couple to deform it locally whilst moving towards its edge. This paper presents this configuration for the first time and develops and verifies an upper bound yield-line model to design stable tool-paths that avoid wrinkling. Raising by spinning is shown to be feasible and more stable than conventional spinning, paving the way for automatic production of deep axisymmetric shapes.

Keywords: sheet metal; forming; spinning

1. Introduction

CNC shear spinning can form conical shells automatically in one roller pass, but when the diameter of the blank must be reduced, multiple passes are required. However, an automatic tool-path design approach applicable to a wide range of shapes is not yet available in industry [1]. Forming parts with cylindrical or re-entrant wall profiles requires complex tooling as well as trial-and-error by experienced operators, with significant waste of time and material. A process that eliminated the tooling and allowed for reliable automation of the roller path would significantly reduce the cost and increase the material efficiency of producing axisymmetric sheet metal parts in small to medium volumes.

Flexible spinning systems with no mandrels have been developed to eliminate the need for part-specific tooling. Shima and colleagues have developed a system with a pair of rollers that grip the workpiece, designed for producing cone-shapes in a one-pass process [2]. Music & Allwood replaced the mandrel with three controllable internal support rollers and succeded in producing cylindrical parts [3]. However the working roller toolpaths were designed by trial-and-error, because roller path design and on-line adjustment using finite element (FE) simultations was still – despite increased computer power – slow and impractical [4]. A major problem is the lack of a reliable prediction of wrinkling. Kong and colleagues have attempted to predict wrinkling as a plastic buckling phenomenon due to compressive circumferential stresses in the flange [5], but their results only help setting the feed ratio, which is not enough for multi-pass spinning.

Yet, deep-drawn shapes have been formed for millennia by craftsmen using hand raising by the hammer (Fig. 1a). As described by Holtzappfel [6], in this craft disks are incrementally formed by experienced workers blowing a hammer on the workpiece just ahead of the contact with an anvil below. The anvil provides the primary reaction force to the hammer blows, and craftsmen hold the workpiece at the opposite edge to both stabilise the piece during blows and rotate it by a small increment after each blow. Using this technique, craftsmen can produce deep axisymmetric shapes with no material wastage and little thickness change.

The flexible spinning system developed by Music & Allwood offers a unique opportunity to replicate the highly localised deformation mechanics of raising by using an internal support roller to provide the principal reaction force at a point much closer to the working roller than in conventional spinning (Fig 1b compared to 1c). How can this new configuration be implemented, and what influence does this have on process stability?

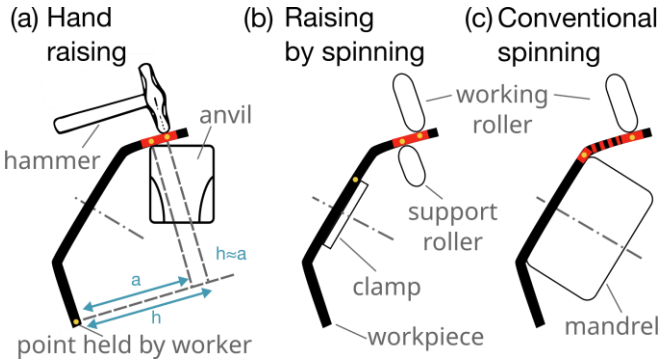

Figure 1. Hand raising compared to raising by spinning and to conventional spinning, showing zones of plasticity in red. Adapted from [6].

2. Process implementation

In the 'raising by spinning' process proposed in this study, one roller is placed on each side of a rotating workpiece (Fig. 2): the Working Roller acts as the hammer while the Anvil Roller acts as the anvil. The rotation of the workpiece and the motion of the rollers along its shape are position-controlled; but uniquely, the displacement into the sheet is force-controlled. This matches the analogy with raising, where impact energy determines the extent of deformation, and importantly – if the maximum allowable force is known – means that 'force-paths' can be designed to avoid wrinkling. Force control has been applied in one-pass shear spinning [7], but no useful force-based approach has been proposed so far for multi-pass spinning.

Both the working roller and the anvil roller are controlled to achieve the same force F normal to the workpiece. The relative size of these forces is important: if the anvil roller force is too large, the roller would 'undo' useful deformation; too low a force would take the mechanics further from that of hand raising, where the forces

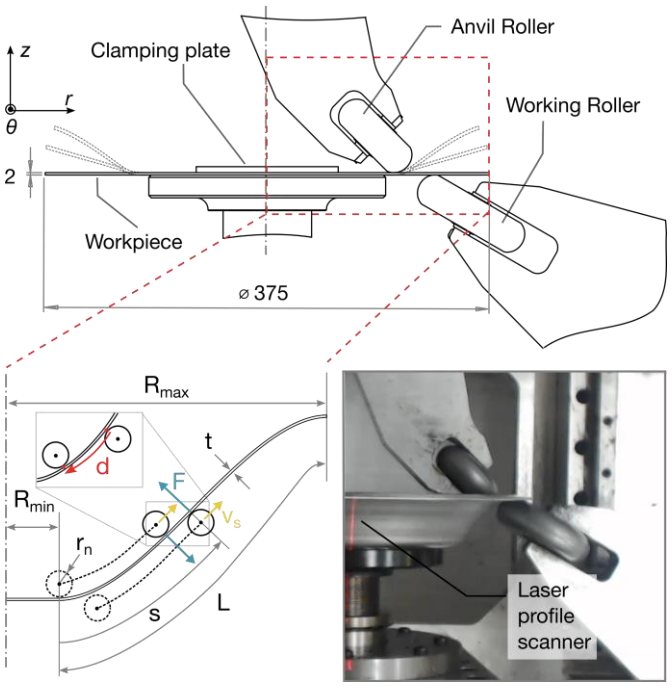

Figure 2. Implementation of raising by spinning and dimensions of the present setup in mm. A couple $C = Fd$ is applied to the workpiece.

are approximately equal (see Fig. 1a, since h ≈ a). Thus, equality of the forces is chosen as a sensible compromise.

The two rollers move on a plane in the radial (r) and axial (z) direction and are synchronised to move towards the edge of the workpiece at a constant velocity along the shape, v_s. This is achieved by scanning the shape of the workpiece at the start of each pass to obtain its 2D profile in (r-z) coordinates. This profile generates a baseline trajectory for each roller: if followed, the rollers would track the workpiece shape without deforming it.

To achieve deformation, a force-path is designed, which prescribes the value of the target force normal to the workpiece surface $F(s) = C(s)/d$ at each position s along the flange, where C is the applied couple and d is the constant offset between the rollers. Then, a displacement x in the direction normal to the workpiece is commanded to achieve the target force F, and a PI control loop is implemented to control the force (Fig. 3), using data from loadcells installed on both axes of both rollers.

Thus, for each roller pass, the user specifies: the velocity v_s of motion in the direction parallel to the workpiece surface, the profile of normal force F to apply at each point s, and the offset d between the rollers. To replicate the mechanics of hand raising, the value of the distance d must be selected carefully: too small a value would replicate the mechanics of ironing, too large a value would make the process more like conventional spinning. A useful reference is the free distance d', i.e. the distance at which the two rollers make no direct contact when they move into the workpiece to apply a force. Based on this definition, we choose to investigate

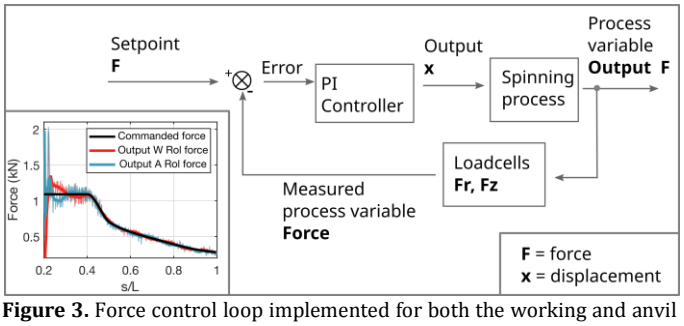

Figure 3. Force control loop implemented for both the working and anvil rollers. The inset shows an example of commanded vs output force profile.

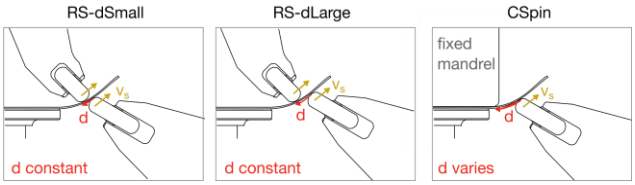

Figure 4. The three process configurations compared in this paper.

two configurations: d = d'/2 (RS-dSmall) and d = d' (RS-dLarge). These are compared to a force-controlled variant of conventional spinning (CSpin), as shown by Fig. 4. All trials presented in this paper are performed on AA1050-H14 blanks with the dimensions reported in Fig. 2, v_s = 1 mm/s and spindle speed = 60 RPM.

3. Prediction of safe force-paths

3.1 Upper bound yield-line model

To avoid using unstable force-paths, wrinkling must be predicted. Instead of modelling wrinkling as a buckling instability, we propose an upper bound plastic collapse model to predict the couple at which yield lines form in the workpiece. This is a common type of structural analysis [8], and it involves calculating the external work and equating it to the internal work dissipated by a hypothetized collapse mechanism.

In this paper, we propose to study the first stages of multi-pass spinning, in which a flat sheet is deformed into increasingly deep curved shells. Therefore, we propose to calculate the collapse couple for two shapes: a flat sheet and a generic curved shell. When a couple is applied to any of these shapes, collapse is observed to occur as a triple fold line pattern (Fig. 5b). If the point couple C, applied at distance R_c from the centre of a disk of radius R_{max}, moves by an angle φ, the external work is $W_{ext} = C\varphi$. This causes a rotation θ at the two side fold lines, and a rotation ψ at the central fold line, so the internal work is given by $W_{int} = m_p(2p\theta + q\psi)$, where m_p is the plastic moment per unit length, p is the length of the side fold lines and q is the length of the central fold line (Fig. 5a). If we assume rigid perfectly plastic material, and we accept the likely overestimate of the resulting collapse load, then $m_p = t^2\sigma_y/4$. Thus, by equating external and internal work, we obtain an expression for the couple $C = t^2\sigma_y/4\varphi\ (2p\theta + q\psi)$. The angle α between the central and side fold lines will take the value that minimises the internal work. If φ is taken to be small and the geometry of the fold lines is solved, expressions for p, q, θ and ψ can be obtained as a function of α, R_c and R_{max} and an expression for C can be written as:

$$C = \left(\frac{\sqrt{R_{max}^2 - R_c^2 \sin^2\alpha}}{\sin\alpha} + \frac{R_{max} - 2R_c}{\tan\alpha} \right) \quad (1)$$

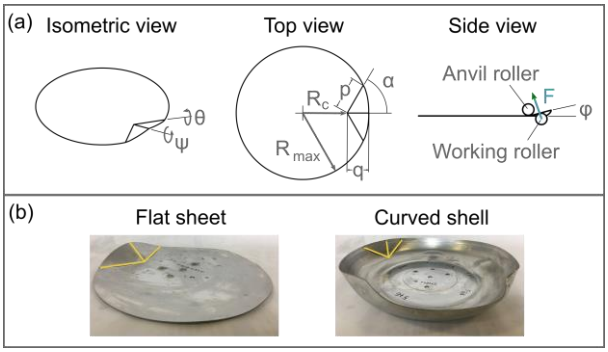

Figure 5. (a) Model of an indented flat sheet, showing the geometrical quantities used; (b) photographs of an indented flat sheet and curved shell, highlighting exemplar triple fold line patterns in each case.

The value of α that minimises the couple is given by:

$$\alpha = \cos^{-1}\left(\frac{(2R_c - R_{max})\sqrt{R_{max}^2 - R_c^2}}{\sqrt{R_{max}^4 - R_c^2R_{max}^2 + 4R_c^3R_{max} - 4R_c^4}}\right) \quad (2)$$

The generic curved shell wall profile is modelled as a circle arc extending over a 90° angle. In this case, the couple is still given by $C = t^2\sigma_y/4\varphi\ (2p\theta + q\psi)$. However, the geometry of the fold lines is too complex for analytical treatment, so the relationship $C(\alpha, R_c, R_{max})$ is found numerically using MATLAB. The next section presents the validation of these analytical predictions using finite element (FE) simulation and experiments.

3.2 Model validation: indentation tests

To validate the upper bound model, indentation tests are performed. The goal of these tests is to obtain a collapse force value for multiple points along the workpiece flange and compare the values to prediction curves obtained using Eqn. 1. Nine tests are performed at regular intervals in s for each of the three process configurations shown in Fig. 4 and each of the two shapes shown in Fig. 5b, for a total of 54 tests.

The test procedure is as follows: with a static workpiece, the rollers are brought in contact with the workpiece surface at the specified location; then, the working roller moves into the workpiece normal to its surface, and the force-displacement curve is measured. The experimental force-displacement curves obtained for the RS-dSmall, RS-dLarge and CSpin configurations from a flat sheet for s/L = 0.6 are plotted as solid lines in Fig. 6a. In the RS-dSmall configuration, the workpiece did not collapse, while in RS-dLarge and CSpin it did, with similar patterns to that shown in Fig. 5b; however, it is difficult to identify the point of collapse from the smooth force-displacement curves. Thus, to gain an insight into the mechanics of the deformation, FE simulations of the indentation tests are performed. Dashed lines in Fig. 6a show that the force in the FE models agrees reasonably well with experimental measurement. To select the value of collapse force, the pattern of plastic dissipation is analysed, as shown in Fig. 7c. The images show that, in the case of RS-dLarge and CSpin, significant plastic deformation occurs away from the area in the immediate vicinity of the tools, which we call the tool zone. Thus, if the rate of plastic dissipation for the whole sheet is broken down

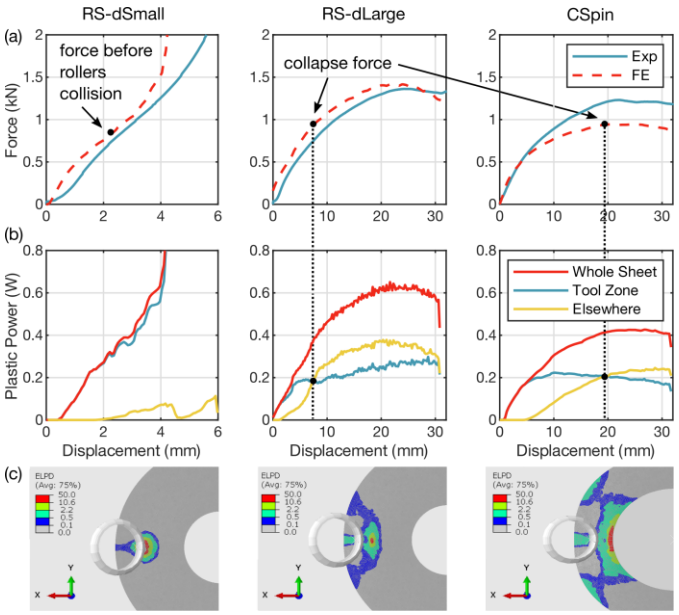

Figure 6. Indentation test results: (a) force-displacement curves for s/L = 0.6 in the experiment and FE for the three process configurations; (b) rate of plastic dissipation for the whole sheet broken down into the tool zone and elsewhere, obtained from FE; (c) the pattern of plastic dissipation (ELPD, units: Nmm) in the FE at the point highlighted in (a) and (b).

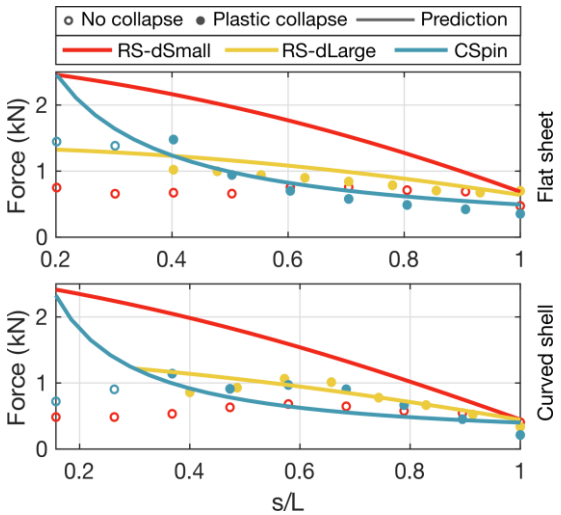

Figure 7. Selected collapse force in the indentation tests as a function of normalised position on the workpiece flange, compared to predictions.

into the tool zone and the rest of the workpiece, the tool zone initially dominates but there is a crossover point beyond which most plastic power is spent away from the tools (Fig. 7b). We choose this point to define collapse, and we select the corresponding force as obtained in the FE simulation. This procedure is repeated for all 54 tests, and the selected collapse forces are plotted in Fig. 7. The plotted prediction curves show the collapse force $F(s/L)$, where $F = C/d$ and $s/L = (R_c+d-R_{min})/L$ as defined in Fig. 2 and 5a, and $C(R_c)$ is given by Eqn. 1. All curves use σ_y = 125 MPa; for the flat sheet t = 2.00 mm while for the curved shell t = 1.43 mm. The figure shows that the highest collapse forces are usually allowed by the RS-dSmall configuration, followed by RS-dLarge and by CSpin. In all configurations, the collapse force lowers towards the edge of the flange. In CSpin, in the small region where the working roller is close to the mandrel (small d and s/L) the predicted collapse force becomes high. The curved shell has higher geometric stiffness but its thickness is lower than the flat sheet, so the collapse force predicted is similar. In the RS-dSmall tests, the rollers collided before the collapse force could be reached: the force before collision is shown as a hollow circle. The results for the flat sheet show good agreement between FE and the analytical model, which should be an upper bound. Whilst the agreement is less strong for the curved shell CSpin configuration, the figure overall suggests that a force-path based on the flat sheet model will be conservative against wrinkling.

4. Spinning tests: the shape effects of raising-by-spinning

In this section, we describe a set of spinning experiments to test two hypotheses: that the upper bound model can predict wrinkling and allow the design of stable force-paths, and that raising by spinning is more stable than conventional spinning. Additionally, the shapes resulting from different force-paths in the three process configurations is investigated.

Three force-paths are tested (Fig. 8): a low force-path, predicted

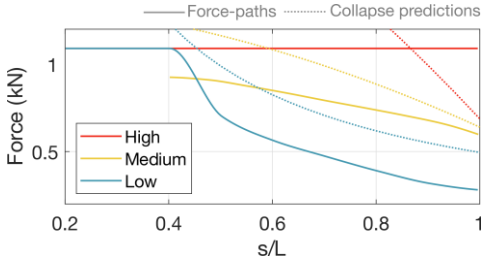

Figure 8. Force-paths used in the spinning tests, compared with plastic collapse predictions for a flat sheet (same curves as top graph of Fig. 7).

to be stable for all process configurations; a medium force-path, stable only for the two RS configurations; and a high force-path, stable only for the RS-dSmall configuration. The low and medium force-paths are designed with values just below the collapse predictions and the experimental results; the high force-path is designed as a flat force line because in the RS-dSmall configuration the rollers collide before the collapse load is reached, so collapse can never occur. For each of the 3 force-paths, the 3 process configurations are tested, for a total of 9 spinning tests. In each test, 10 tool-passes with the same force-path are performed; failure or success is reported, and the shapes and thickness profiles of the parts are measured.

The results of the tests are presented in Fig. 9. The figure shows that raising by spinning can successfully produce deep axisymmetric shapes with a range of wall profiles. Moreover, the predictions made by the model proved correct: wrinkling occurs in CSpin when using the medium and high force-path; and it also occurs in RS-dLarge when using the high force-path. All other experiments avoided wrinkling – or any other failure. When the high force-path was used with RS-dSmall, an unexpected process limit occurred: to keep a high force towards the end of the flange, the anvil roller attempted to push the workpiece 'backwards', i.e. to form it in the direction opposite to conventional tool motion and beyond hardware limits. Therefore, this trial was stopped early.

The workpiece shapes and the thickness profiles of the 5 successful parts (green boxes in Fig. 9) are shown in Fig. 10 and Fig. 11 respectively. The shapes are referenced against the wall profile of a 90° cylinder. To compare the extent of deformation quantitatively, the value A of the (r-z) area swept by the deformed workpiece flange is given as a proportion of that swept by the wall profile of a 90° cylinder. Low force-paths lead to concave or conical

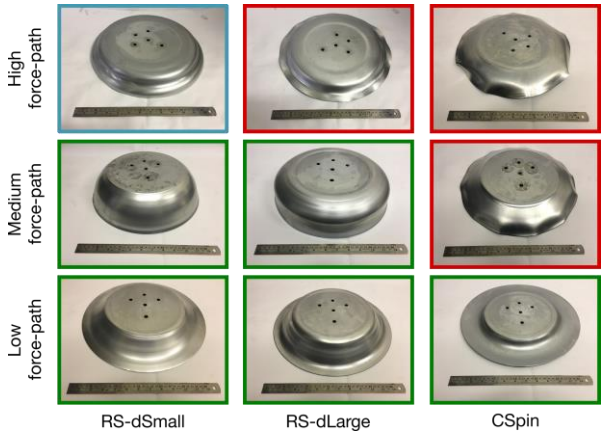

Figure 9. Results of the spinning tests: green boxes indicate success, red boxed indicate wrinkling and the light blue box indicates that a geometrical limit was reached. The ruler is 30 cm long.

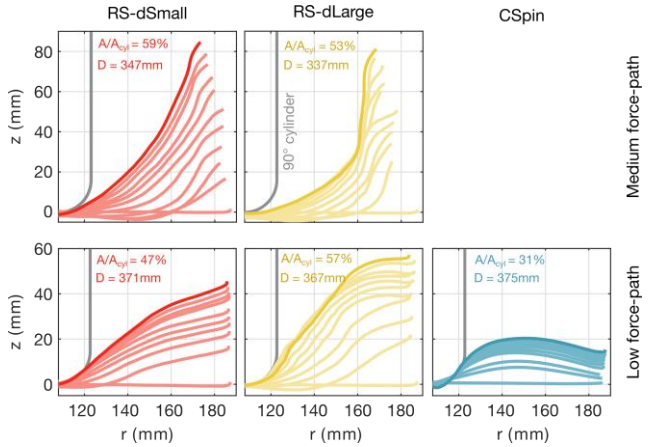

Figure 10. Workpiece shapes achieved after each pass in the spinning tests. The final part diameter and the extent of deformation are also given.

wall profiles, while medium force-paths push further towards the edge of the flange, thus leading to convex wall profiles and a more significant reduction in diameter. As the shape deforms, its stiffness increases and each roller pass leads to less change in shape; this suggests that further passes should apply a force-path with higher mean force. The thickness profiles of Fig. 11 demonstrate that raising by spinning leads to patterns very similar to conventional spinning. Relative to the extent of deformation in each trial, the RS-dLarge configuration with the low force-path led to the best result (57% deformation while retaining 60% of the original thickness). Medium force-paths lead to higher thinning than low force-paths without deforming the shape much further; however, they lead to a greater diameter reduction.

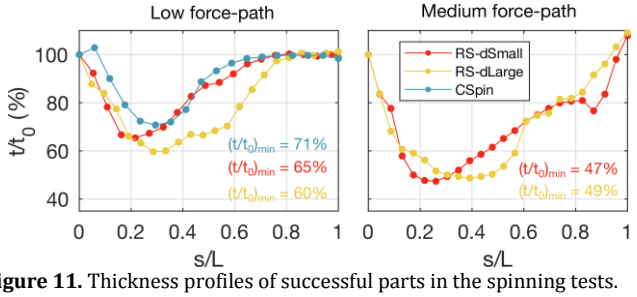

Figure 11. Thickness profiles of successful parts in the spinning tests.

5. Conclusions

The rollers of a of flexible spinning system were controlled to replicate the ancient process of raising for the first time. The novel process configuration allowed the production of deep axisymmetric shapes with no dedicated tooling and comparable thinning to conventional spinning. Force control was used for the first time in multi-pass spinning. This enabled a new way to avoid wrinkling by using an upper bound yield-line model to predict the maximum allowable force. The results confirm the predictions and show the promise of a stable process, with roller pass sequences that are easy to design. This is true not only for raising by spinning, but also for conventional spinning. Thus, the results presented in this paper pave the way towards automation of the spinning process. The choice of force-path influences the shape taken by the workpiece; in future work, the implementation of a position-based virtual mandrel can be tested to limit motion of the rollers and achieve the shape set by part designers.

Acknowledgements

IMR is supported by a studentship provided by the UK's Engineering and Physical Sciences Research Council (EPSRC); CJC and JMA are supported by EPSRC grant EP/S019111/1 awarded to JMA. EGL is supported by EPSRC grant EP/S515760/1. IMR would like to thank Verónica Salazar for help with the analytical model.

References

[1] Music, O., Allwood, J.M., Kawai, K., 2010. A review of the mechanics of metal spinning. J. Mat. Proc. Tech. 210, 3–23.
[2] Shima S, Kotera H, Murakami H., 1997. Development of Flexible Spin-Forming Method. Journal of the JSTP 38(440):814–8.
[3] Music, O., Allwood, J.M., 2011. Flexible asymmetric spinning. CIRP Ann. – Manuf. Technol. 60, 319–322.
[4] Polyblank J.A., 2015. The Mechanics and Control of Flexible Asymmetric Spinning (PhD Thesis), University of Cambridge.
[5] Kong Q., Yu Z., Zhao Y., Wang H., Lin Z., 2017. Theoretical prediction of flange wrinkling in first-pass conventional spinning of hemispherical part, J. of Mat. Proc. Tech., 246, 56-68.
[6] Holtzapffel, C., 1852. Turning and Mechanical Manipulation: Intended as a Work of General Reference and Practical Instruction, on the Lathe, and the Various Mechanical Pursuits Followed by Amateurs (Vol. 1).
[7] H. Arai, 2006. "Force-controlled metal spinning machine using linear motors," Proc. 2006 IEEE Int. Conf. on Robotics and Automation, Orlando, FL, pp. 4031-4036.
[8] Save, M.A. & Massonnet, C.E., 1972. Plastic analysis and design of plates, shells and disks., Amsterdam: North-Holland.